OPTICAL PROPERTIES OF INDIUM

A. I. GOLOVASHKIN, I. S. LEVCHENKO, G. P. MOTULEVICH, and A. A. SHUBIN

P. N. Lebedev Physics Institute, Academy of Sciences, U.S.S.R.

Submitted to JETP editor June 23, 1966

J. Exptl. Theoret. Phys. (U.S.S.R.) **51**, 1622–1633 (December, 1966)

The optical properties of indium are measured from 0.55 to 10 μ at 4.2° and 295° K. The following microscopic properties pertaining to conduction electrons are determined: conduction electron concentration, frequency of electron collisions, mean electron velocity on the Fermi surface, and the total area of the Fermi surface. The following characteristics of interband transitions are determined: the Fourier coefficients of the pseudopotential, the threshold frequencies of interband transitions, and the frequency dependence of absorption near threshold. Relationships between the two groups of properties are established and the temperature dependences of the properties are determined.

1. INTRODUCTION

THE present work continues the investigation of the optical properties of polyvalent metals at the Optical Laboratory of the Lebedev Physics Institute. The influence of the static lattice potential on the conduction electron concentration N_{opt} has recently been ascertained using an optical method. In [1] simple relations were obtained between the difference $N_{val} - N_{opt}$ and the Fourier coefficients (components) of the pseudopotential (N_{val} is the concentration of valence electrons). In lead this difference is maintained by the pseudopotential. The same evidently will also apply to tin, but in aluminum the experimentally observed difference considerably exceeds the calculated value. It was therefore of interest to investigate indium, which is also in the third group.

The Fourier components of the pseudopotential are known from experimental investigations of the de Haas–van Alphen effect,[2,3] but they are not known for indium, and we assume that they should be derived from optical measurements. For this purpose the optical constants of indium must be measured over a broad spectrum at sufficiently low temperatures. In the present work the optical properties of indium were investigated in detail for the infrared and visible regions of the spectrum at both room and helium temperatures; properties of the conduction electrons and interband transitions were thus derived. Measurements performed at two temperatures made it possible to determine the temperature dependences of these properties.

2. EXPERIMENT

A. Our method of measuring the optical constants n and κ (of the complex refractive index $n - i\kappa$) has been described in earlier papers.[4-7] The measurements at room temperature, were performed with two experimental setups;[4-7] the results agreed within 0.5%. The measurements at helium temperature were performed with the apparatus described in [7]. In all instances the measurements covered the spectral interval 1–10 μ, a germanium bolometer being used as the detector.

The optical constants of indium were also measured at wavelengths 0.55–2.6 μ using a monochromator with glass optics and a Soleil-Babinet quartz compensator, wherewith the phase difference between the s and p components of light reflected from the investigated mirrors was reduced to an odd multiple of $\pi/2$ (with 2′ accuracy). The radiation detectors were a photoconductive cell at 0.8–2.6 μ and a photomultiplier at 0.55–1.2 μ.

The sensitivity regions of the three detectors (bolometer, photoconductive cell, and photomultiplier) overlapped, yielding identical values of n and κ in the overlapping regions.

B. The experimental samples were prepared by condensing indium vapor in a vacuum on polished glass surfaces. The indium was evaporated from tantalum boats at about 150 Å/sec under a pressure of $(2–5) \times 10^{-6}$ Torr. We used a new method of preparing indium mirrors, which was developed in the Optical Laboratory by A. A. Shubin and will be published separately.

The films were 0.3–0.4 μ thick, with 90 ± 4% of the density of bulk metal, and exhibited conduc-

Table I. Optical constants of indium

λ, μ	T = 295° K		T = 4,2° K		λ, μ	T = 295° K		T = 4,2° K	
	n	κ	n	κ		n	κ	n	κ
10	24.8	51,9	13 5	62,3	1,6	2,33	11,8	1.48	11.9
8	18.4	45.3	7,5	50,6	1,55	—	—	1.45	11.45
6	12.4	37,2	4,2	38.7	1,5	2,19	11.0	1,39	10.9
5	9.77	32.2	3.1	32.7	1.45	—	—	1.36	10.6
4	7,27	26,7	2,3	26.7	1,4	2.06	10.35	1.35	10,3
3.5	6.00	23.9	2.05	23.9	1,35	—	—	1,32	9.95
3,0	4,70	20.9	1.90	20,9	1,3	1,95	9,70	1,30	9.60
2.6	4.0	18,3	1.92	18.25	1.25	—	—	1.28	9.24
2,55	—	—	1.93	17.8	1,2	1.87	9.00	1.28	8.88
2,50	3,81	17,6	1,95	17,5	1,15	—	—	1,31	8,42
2.45	—	—	1,97	17,2	1.1	1.84	8.38	1,35	8.00
2.4	3.65	16.9	1,99	16.8	1,05	—	—	1.41	7.60
2.35	—	—	2.00	16.5	1,0	1.81	7.77	1.49	7.25
2.3	3,48	16.3	2,00	16.2	0,95	1.72	7.44	1.65	7,00
2.25	—	—	1,99	16.0	0,9	1,59	7.18	1.73	6,85
2.2	3,30	15,6	1.98	15,6	0,85	1,45	6.78	1.71	6.72
2.15	—	—	1.96	15.3	0,82	—	—	1.65	6.68
2.1	3,13	15.0	1.92	15.0	0.8	1,32	6,60	1.59	6,65
2.05	—	—	1,88	14,8	0,76	1,19	6,31	1.33	6,50
2,0	2,97	14,5	1.84	14.6	0,75	1.17	6,26	1.26	6 45
1.93	—	—	1.78	14.2	0,74	1,13	6,18	1.20	6,40
1.9	2,80	13,8	1,75	13,8	0,72	1,07	6,00	1.09	6,20
1.85	—	—	1.70	13,55	0,7	1,01	5,83	0.99	6,00
1.8	2,64	13,1	1,65	13,2	0,65	0.90	5,42	0.835	5.50
1.75	—	—	1.61	12.9	0.6	0.795	5,02	0.77	5,08
1.7	2 49	12,5	1,56	12.6	0.55	0,70	4.70	0.695	4.70
1.65	–	—	1.52	12,2					

tivity at 295° K which was 97% of the bulk-metal conductivity. The ratio of the conductivities at liquid nitrogen temperature and room temperature was 4.52, while the ratio for bulk metal is 5.02.[8] The residual resistance was 3% of the resistance at room temperature. The superconducting transition temperature was 3.40° K, which agrees with the transition temperature of the bulk metal.[9] The superconducting transition width varied from 0.004 to 0.06° K for different samples, indicating good homogeneity of the films, which possessed specular surfaces of high quality. The foregoing properties show that our present method of preparation produced indium films having properties close to those of the bulk metal.

In previous investigations[10, 11] the optical properties of the indium films differed more strongly from those of the bulk metal. In [10] an interlayer made of lead contaminated the sample slightly through diffusion. The density and conductivity of the films comprised 81% and 64%, respectively, of the corresponding bulk-metal properties. In [11] the films were deposited on a cooled substrate. The properties of these films were not reported. However, it is known[12] that this method of preparation produces a finely dispersed structure in the film.

3. EXPERIMENTAL RESULTS

The measurements of the optical constants n and κ are given in Table I and in Figs. 1 and 2. In calculating these constants we used formulas of [6] to take into account the dependence of surface impedance on the angle of incidence. In both the visible and infrared regions κ was determined with 1% accuracy; however, the error increased to 1.5–2% at the edges of the investigated spectral interval. In most of this interval n was also determined with 1% accuracy; the error increased to 2–3% at the edges. The same figures show the results obtained in [10, 11] at room temperature alone. In [10] the spectral interval was 1–10 μ, while in [11] it was 0.475–2 μ. Figures 1 and 2 also show that the results in [10] are close to those in the present work. However, our results differ much more from those given in [11], thus confirming that a metal deposited on a cold substrate differs from the bulk metal in its structure.

The curves in Fig. 1 exhibit two distinct maxima at helium temperature, at 0.8–0.9 μ and 2–2.5 μ. At room temperature only a small change in the slope of the curve appears at about 1 μ.

The table and the figures indicate considerable temperature dependence for n over the entire region. On the other hand, in the region 1.3–4.5 μ no temperature dependence of κ is observed; however, at longer wavelengths κ is considerably larger for 4.2° K than for room temperature. The corresponding values of κ also differ in the region 0.7–1.2 μ. The results will now be treated in detail.

4. TREATMENT OF EXPERIMENTAL DATA

A. We shall first analyze the measurements in the longer wavelength region of the spectrum, where the optical constants are determined by the

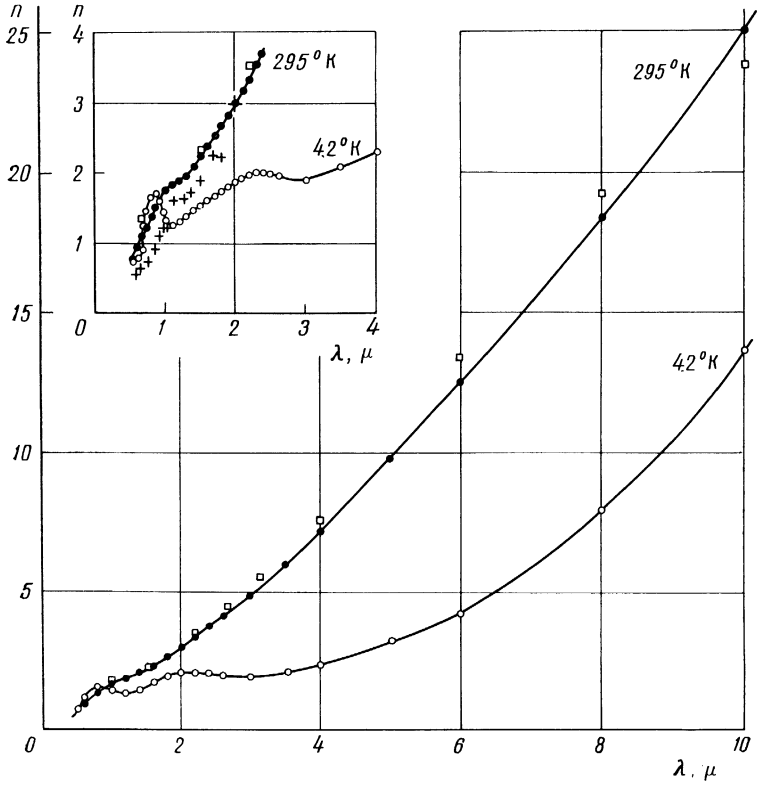

FIG. 1. Real part of the complex refractive index vs wavelength of light at two temperatures. ●, ○ – present work, □ – [10], + – [11].

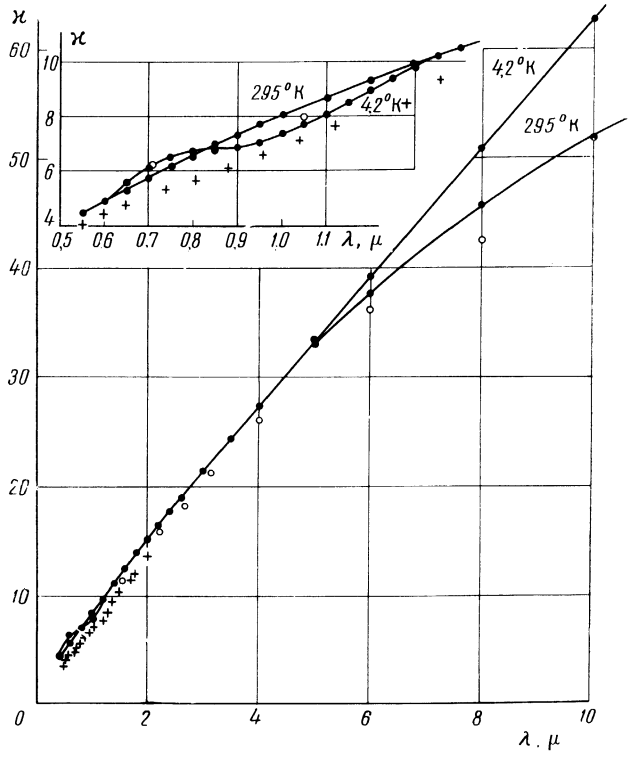

FIG. 2. Imaginary part of the complex refractive index vs wavelength of light at two temperatures. ● – present work, ○ – ref. [10], + – ref. [11].

conduction electrons. Our results show a weak anomalous skin effect in this region. Indeed, even at helium temperature the surface loss does not exceed 25% of the total loss.

According to the results obtained by one of the present authors[13] for the weak anomalous skin effect it is reasonable to use the relations

$$N_{\text{opt}} = \frac{0{,}1115 \cdot 10^{22}\varkappa^2}{\lambda^2} \frac{(1+n^2/\varkappa^2)^2}{1-n^2/\varkappa^2} \frac{1}{1-\beta_1}, \tag{1}$$

$$\nu = \frac{3.767 \cdot 10^{15}}{\lambda} \frac{n/\varkappa}{1-n^2/\varkappa^2} \frac{1-\beta_2}{1-\beta_1}, \tag{2}$$

$$\beta_1 = \frac{3}{8} \frac{\langle v_F \rangle}{c} \varkappa \frac{(1+n^2/\varkappa^2)(\nu/\omega - n/\varkappa)}{(1+\nu^2/\omega^2)(1-n^2/\varkappa^2)}, \tag{3}$$

$$\beta_2 = \frac{3}{16} \frac{\langle v_F \rangle}{c} \varkappa \frac{1+n^2/\varkappa^2}{n/\varkappa} \frac{1+(n/\varkappa)(\nu/\omega)}{1+\nu^2/\omega^2}; \tag{4}$$

here λ is the wavelength of light in microns, $\omega = 1.88 \times 10^{15}/\lambda$ is the angular frequency of light in sec^{-1}, ν is the effective frequency of collisions between electrons, $\langle v_F \rangle$ is the average velocity of electrons on the Fermi surface, and c is the velocity of light.

The corrections β_1 and β_2 take the character of the skin effect into account. We shall see subsequently that this effect is considerably smaller

than unity, thus permitting the use of (1)–(4). The calculation of the latter requires knowledge of $\langle v_F \rangle$, which should be obtainable from the same optical measurements. We shall describe how this can be done.

Gurzhi and one of the present authors[1] have shown that, to first-order terms in $|V_g|/E_F$, the periodic potential of the lattice does not affect the density of states at the Fermi surface. (V_g is a Fourier component of the pseudopotential, the subscript g denotes the corresponding reciprocal-lattice vector, and E_F is the Fermi energy.) It follows that

$$S_F^0 / v_F^0 = S_F \langle v_F^{-1} \rangle. \tag{5}$$

For cubic metals we have

$$N_{opt} / N_{val} = S_F \langle v_F \rangle / S_F^0 v_F^0. \tag{6}$$

In (5) and (6), S_F° is the surface area of the Fermi sphere for free electrons with the concentration N_{val}, v_F° is the velocity of these electrons on the Fermi surface, and S_F is the area of the true Fermi surface.

Assuming $\langle 1/v_F \rangle \approx 1/\langle v_F \rangle$, we obtain from (5) and (6)

$$\frac{S_F}{S_F^0} \approx \frac{\langle v_F \rangle}{v_F^0} \approx \left(\frac{N_{opt}}{N_{val}} \right)^{1/2}. \tag{7}$$

This formula can be used to determine $\langle v_F \rangle$ with a small error of about 2–3% that has practically no effect on our results, since the correction terms containing $\langle v_F \rangle$ are small.

On the basis of the foregoing discussion we propose the following scheme for treating the experimental results. Utilizing the method of successive approximations, we set $\beta_1 = \beta_2 = 0$ in zeroth approximation. We then determine N_{opt} and ν in zeroth approximation. We use (7) to determine the first approximation for $\langle v_F \rangle$, calculate β_1 and β_2 in the same approximation, and then use these values to calculate N_{opt} and ν in first approximation. This process converges rapidly.

Table II and Figs. 3 and 4 show our results for indium. The values of β_1 and β_2 in the table are indeed small; thus the skin effect is only weakly anomalous. It is also seen that at 5–10 μ for room temperature and 4–10 μ for helium temperature the value of N_{opt} derived from (1) is independent of λ. Therefore we can take the mean values of N_{opt} in these intervals. In about the same spectral intervals ν, β_1/λ^2, and β_2 also become constants. The mean values of these quantities and of N_{opt} in the indicated intervals are given in Table III, which also contains other microproperties of indium.

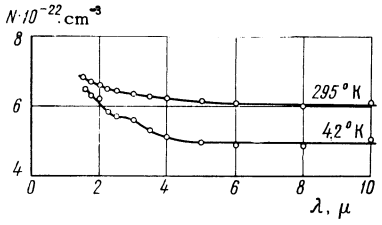

FIG. 3. Dependence of $N_{opt} = \frac{0{,}1115 \cdot 10^{22}}{\lambda^2} \frac{(n^2+\varkappa^2)^2}{\varkappa^2 - n^2} \frac{1}{1-\beta_1}$

In the regions 5–10μ for T = 295°K and 4–10μ for T = 4.2°K this quantity gives the concentration of conduction electrons.

The average velocity $\langle v_F \rangle$ on the Fermi surface was calculated from (7). In calculating the frequency of electron-phonon collisions (ν_{ep}), the classical frequency of electron-phonon collisions (ν_{ep}^{cl}), the frequency of electron collisions with impurities and defects (ν_{ed}), the electron mean free path (l), and the skin thickness (δ) we used the following relations:

$$\nu = \nu_{ep} + \nu_{ed},$$

$$\nu_{ep}^{cl} + \nu_{ed} = \frac{e^2}{m} \frac{N_{opt}}{\sigma_{st}}, \qquad \frac{\nu_{ed}}{\nu_{ep}^{cl} + \nu_{ed}} = \frac{R_{res}}{R},$$

$$l = \frac{\langle v_F \rangle}{\nu}, \qquad \delta = \frac{\lambda}{2\pi\varkappa}, \tag{8}$$

where e and m are the free-electron charge and mass, σ_{st} is the static conductivity at the temperature T, and R_{res}/R is the ratio of the residual resistance to the resistance at the temperature T.

B. The treatment of the results at shorter wavelengths was more complicated because the optical constants here depend on both the conduction electrons and interband transitions. By utilizing the additivity of the complex dielectric constant

$$\varepsilon' = (n - i\varkappa)^2 = \varepsilon - i \frac{4\pi\sigma(\omega)}{\omega},$$

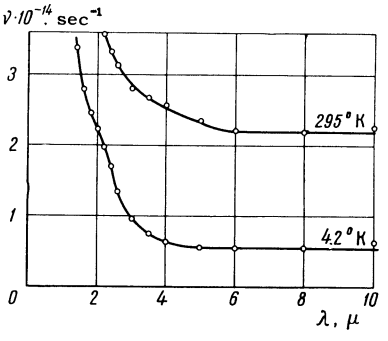

FIG. 4. Dependence of ν on λ at different temperatures.

Table II. Dispersion of N_{opt}, ν, β_1, and β_2 for indium

λ, μ	$T = 295°$ K				$T = 4.2°$ K			
	$10^{-22} N_{opt}$ cm^{-3}	$\nu \cdot 10^{-14}$, sec^{-1}	$\beta_1 \cdot 10^2$	$\beta_2 \cdot 10^2$	$10^{-22} N_{opt}$ cm^{-3}	$\nu \cdot 10^{-14}$, sec^{-1}	$\beta_1 \cdot 10^2$	$\beta_2 \cdot 10^2$
10	6.11	2.26	3.88	6.83	5.04	0.669	1.29	20.6
8	5.98	2.18	2.80	7.65	4.79	0.541	0.59	24.6
6	6.06	2.20	1.82	8.14	4.82	0.514	0.31	25.7
5	6.16	2.35	1.42	7.87	4.91	0.543	0.23	24.8
4	6.26	2.59	1.05	7.38	5.09	0.636	0.19	22.3
3.5	6.32	2.70	0.86	7.23	5.32	0.745	0.18	20.0
3	6.33	2.78	0.67	7.12	5.56	0.963	0.19	16.5
2.6	6.40	3.13	0.58	6.42	5.69	1.35	0.21	12.4
2.55	—	—	—	—	5.64	1.43	0.22	11.7
2.5	6.39	3.23	0.55	6.24	5.68	1.51	0.22	11.2
2.45	—	—	—	—	5.73	1.60	0.23	10.7
2.4	6.39	3.36	0.53	6.00	5.71	1.70	0.23	10.1
2.35	—	—	—	—	5.76	1.78	0.24	9.71
2.3	6.45	3.47	0.50	5.86	5.80	1.87	0.24	9.36
2.25	—	—	—	—	5.92	1.93	0.24	9.17
2.2	6.44	3.60	0.48	5.66	5.90	2.02	0.24	8.76
2.15	—	—	—	—	5.94	2.09	0.24	8.51
2.1	6.51	3.72	0.46	5.52	5.99	2.14	0.23	8.35
2.05	—	—	—	—	6.11	2.18	0.23	8.30
2.0	6.67	3.82	0.43	5.45	6.24	2.22	0.22	8.25
1.93	—	—	—	—	6.34	2.29	0.22	8.07
1.9	6.68	3.99	0.41	5.23	6.23	2.35	0.22	7.80
1.85	—	—	—	—	6.24	2.41	0.21	7.63
1.8	6.69	4.19	0.39	5.00	6.30	2.46	0.20	7.52
1.75	—	—	—	—	6.36	2.53	0.20	7.36
1.7	6.81	4.39	0.37	4.83	6.42	2.59	0.19	7.25
1.65	—	—	—	—	6.40	2.69	0.19	6.97
1.6	6.84	4.63	0.34	4.60	6.47	2.78	0.19	6.81
1.55	—	—	—	—	6.40	2.93	0.18	6.43
1.5	6.77	5.00	0.32	4.25	6.19	3.06	0.18	6.08

Table III. Microproperties of indium

Quantity	$T = 295°$ K	$T = 4.2°$ K	Quantity	$T = 295°$ K	$T = 4.2°$ K
$N_a \cdot 10^{-22}$, cm^{-3}	3.45±0.14	3.45±0.14	$\nu \cdot 10^{-14}$, sec^{-1}	2.25±0.06	0.58±0.06
$N_{opt} \cdot 10^{-22}$, cm^{-3}	6.08±0.06	4.93±0.1	$\nu_{ep} \cdot 10^{-14}$, sec^{-1}	2.20±0.06	0.54±0.06
N_{opt}/N_a	1.76	1.43	$\nu_{ep}^{cl} \cdot 10^{-14}$, sec^{-1}	1.58±0.06	—
$(\beta_1/\lambda^2) \cdot 10^4$, μ^{-2}	4.75±0.60	1.03±0.16	$\nu_{ed} \cdot 10^{-14}$, sec^{-1}	0.05	0.04
$\beta_2 \cdot 10^2$	7.6±0.4	23.6±1.7	$l \cdot 10^6$, cm	0.6	2.0
$\langle v_F \rangle \cdot 10^{-8}$, cm/sec	1.28±0.04	1.16±0.03	$\delta \cdot 10^6$, cm	2.5	2.4

Here N_a is the concentration of atoms.

we can separate the two different contributions. The conduction electron contribution can be determined from the previously derived microproperties.

The quantity of greatest interest is

$$\sigma(\omega) = \sigma_1(\omega) + \sigma_2(\omega). \tag{9}$$

Here σ_1 pertains to the conduction electrons and σ_2 to the interband transitions.

The value of σ_1 in this region was determined from the formulas

$$\sigma_1 = \frac{e^2 N_{\text{opt}} \nu}{m(\omega^2 + \nu^2)}(1 - \alpha), \qquad \alpha = \beta_2 + \frac{2\omega^2}{\omega^2 + \nu^2}(\beta_1 - \beta_2). \tag{10}$$

Here N_{opt}, ν, β_1/λ^2, and β_2 are the mean values obtained for the longer wavelength region (Table III); they also determine the contribution made by free electrons to $\sigma(\omega)$ and the other optical constants at shorter wavelengths.

The quantity σ_2 was defined as the difference between the experimental values $\sigma(\lambda)$; the results for $\sigma_2(\lambda)$ are shown in Fig. 5. It must be mentioned that at helium temperature the free electrons make only a small contribution to σ; therefore the part associated with interband transitions can be discriminated quite accurately. At room temperature the conductivity σ_1 is larger, so that σ_2 is determined less accurately. Figure 5 shows two pronounced maxima at helium temperature; these correspond to the wavelengths $\lambda_1 = 0.84 \pm 0.01\mu$ and $\lambda_2 = 2.1 \pm 0.1\mu$. At room temperature the shorter-wavelength peak is still observed, but its location is shifted to $\lambda_1' = 1.00 \pm 0.02\mu$. The curve of $\sigma(\lambda)$ then also exhibits a slight rise in the

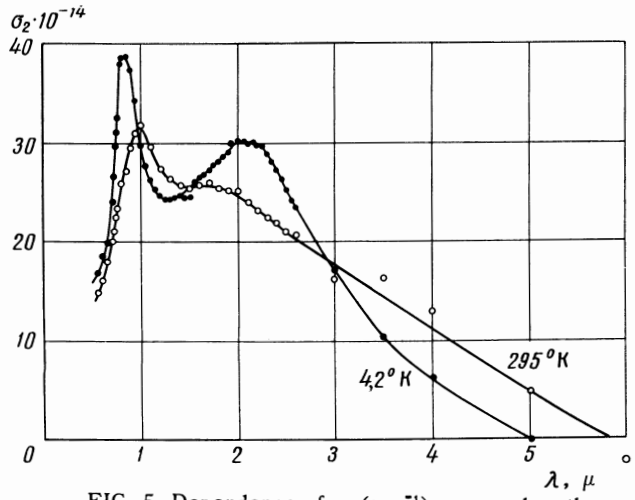

FIG. 5. Dependence of σ_2 (sec^{-1}) on wavelength. ●– T = 4.2°K, ○– T = 295°K.

1.5–3μ region, but the location of the second maxima cannot actually be determined, since it is low and broad and is located on a slope of the first peak. The same figure shows that the wavelength corresponding to the threshold for interband transitions is $5.00 \pm 0.25\,\mu$ at helium temperature and $5.8 \pm 0.6\,\mu$ at room temperature. The indicated errors pertain to measurements of the parameters of the conduction electrons.

The separation $\epsilon = \epsilon_1 + \epsilon_2$ can be made similarly, but the interpretation of the rises on the corresponding curve is then more complicated.

5. DISCUSSION OF RESULTS

A. The results obtained for the temperature dependence of ν show that this dependence for indium is of the same character as for tin and lead.[6,14] Even at the temperature of liquid helium ν remains large; Table III gives $\nu(T = 4.2°K) = 5.8 \times 10^{13}$ sec^{-1}.

We recall that ν contains no contribution associated with the surface loss, which is taken into account by the correction β_2. The error in ν that results from inaccuracy in determining β_2 is unimportant, since the total surface loss is not large and comprises $\approx 24\%$ at helium temperature. Most of ν is contributed by electron-phonon collisions, since $\nu_{ep} \gg \nu_{ed}$. The large value of ν_{ep} at helium temperature is associated with the quantum effect calculated by Gurzhi and by Holstein,[15,16] which we observed experimentally for the first time in tin and lead.[6,14]

The theory predicts $\nu_{ep}(0)/0.94\,\nu_{ep}(\Theta) = 0.4$, where Θ is the Debye temperature obtained from the temperature dependence of the resistance. From our values for ν_{ep} at T = 295° and 4.2°K in conjunction with the temperature-dependent behavior of the static conductivity of our samples, we obtain

$$\nu_{ep}(0) / 0.94\nu_{ep}(\Theta) = 0.39,$$

which agrees well with the theoretical value of this quantity.

B. Before proceeding to calculate the effect of the static lattice potential of indium on its optical properties we should recall that indium is a trivalent metal with a face-centered tetragonal lattice having the axial ratio 1.077. For this lattice the only important Fourier components of the pseudopotential are V_{111}, $V_{200} = V_{020}$, and V_{002}.[2,3,17] We also have $V_{200} \approx V_{002}$ because the lattice deviates only very slightly from the cubic type. The potential has only eight components for the [111] direction, and six for the [200] direction. On the basis of the data for aluminum we can assume that V_{111} will differ greatly from V_{200}; this should be manifested by two rises on the $\sigma(\lambda)$ curve. We can expect that near $\hbar\omega = 2V_g$, where g represents either (111) or (200), the loss function will have a maximum that is proportional to σ. Indeed, only at these energies are nonphonon-assisted transitions possible for a very large number of electrons whose moments are determined by the regions where the corresponding Bragg planes intersect the Fermi surface. With increasing wavelength of light there is a substantial decrease in the number of electrons for which an interband transition is allowed by energy conservation. At shorter wavelengths the great bulk of the electrons can make transitions only with the participation of phonons. On this basis we assume that the Fourier components of the pseudopotential can be determined from the maxima of $\sigma(\lambda)$.

From the results given in Fig. 5 for helium temperature we obtain two values, 0.74 and 0.30 eV, of the Fourier coefficients of the pseudopotential. By analogy with aluminum we can expect to have $|V_{200}| > |V_{111}|$; therefore we assume $|V_{111}| = 0.30$ eV and $|V_{200}| = 0.74$ eV.

Measurements of the optical constants at different temperatures enabled us to determine the temperature dependence of the potential V_{200}; Fig. 5 indicates $V_{200}(T = 295°K) = 0.62$ eV. The ratio of the potentials at the different temperatures is $V_{200}(4.2°K)/V_{200}(295°K) = 1.19$. Unfortunately, V_{111} cannot be determined at room temperature.

One of the present authors has considered the temperature dependence of the pseudopotential Fourier coefficients V_g in [18], where he showed that for each V_g the thermal vibrations of the lat-

Table IV. Electron properties derived by two different methods

Quantity	From the parameters of conduction electrons	From the parameters of the pseudopotential
N_{opt} ($T = 4.2°$ K)/N_a	1.43	1.55(from(11))
N_{opt} ($T = 295°$ K)/N_{opt} ($T = 4.2°$ K)	1.23	1.15(from(11))
S_F/S_F^0	0.69(from(7))	0.72(from(7). (11)) 0.70(from(12))
$\langle v_F\rangle/v^0{}_F$	0.69(from(7))	0.72(from(7). (11)) 0.74(from(6))

tice lead to a temperature-dependent factor that coincides with the corresponding Debye–Waller factor. This factor determines the temperature dependence of the diffraction maximum intensities in the lattice. With increasing temperature the Fourier coefficients of the pseudopotential should decrease; this is observed experimentally.

C. The effect of the lattice potential on N_{opt}, S_F, and v_F has been considered in [1]. N_{opt} for indium can be determined from

$$\frac{N_{val}-N_{opt}}{N_{val}} = 4.84\frac{|V_{111}|}{E_F^0}\left(\frac{1}{2}+\frac{\varphi_{111}}{\pi}\right) + 4.18\frac{|V_{200}|}{E_F^0}\left(\frac{1}{2}+\frac{\varphi_{200}}{\pi}\right), \quad (11)$$

$$\varphi_{111} = \tan^{-1}\frac{0.355E_F^0}{|V_{111}|}, \quad \varphi_{200} = \tan^{-1}\frac{0.199E_F^0}{|V_{200}|}. \quad (11a)$$

Here E_F^0 is the Fermi energy for the free-electron sphere of all valence electrons; $E_F^0 = 8.6$ eV for indium.

S_F for indium can be determined from

$$\frac{S_F^0 - S_F}{S_F^0} = 4\frac{|V_{111}|}{E_F^0}f\left(\frac{p_{111}}{p_F^0}\right) + 3\frac{|V_{200}|}{E_F^0}f\left(\frac{p_{200}}{p_F^0}\right), \quad (12)$$

$$f(z) = z^{-1}E(z) - (z^{-1} - z)K(z), \quad (12a)$$

where K and E are complete elliptic integrals of the first and second kinds. The average velocity $\langle v_F\rangle$ can be determined from (6).

Table IV gives the values of N_{opt}, S_F, and $\langle v_F\rangle$ derived from the given formulas. In calculations based on (11), (12), and (6) the error is approximately $|\bar{V}_g|/E_F^0$, which is about 6% for indium.

In Table IV we compare several electron properties derived by two different methods; the values in the first column were obtained only from the parameters of the conduction electrons, while those in the second column were obtained from the parameters of the pseudopotential. The former were derived using results pertaining to the longer wavelengths of the spectrum, and the latter for the shorter wavelengths. In calculating the temperature dependence of N_{opt} using the pseudopotential coefficients we assumed identical temperature dependences of V_{111} and V_{200}. This cannot lead to a large error because V_{200} makes the main contribution to the difference $N_{val} - N_{opt}$.

Table IV shows that the properties derived by the two methods are in good agreement.[1)] This confirms first, the correctness of considering the effect of the pseudopotential on electron properties in indium and, secondly, the fact that optical measurements provide the most direct means of determining the Fourier coefficients of the pseudopotential.

The closeness of the values of N_{opt}/N_a derived by the two methods shows that the difference $N_{val} - N_{opt}$ for indium depends mainly on the static lattice potential.

For indium we observe a relatively large temperature dependence of N_{opt}, which is accounted for by the temperature dependence of the pseudopotential Fourier coefficients; N_{opt} increases with rising temperature. The result obtained for indium agrees with the result for other polyvalent metals.[6, 14, 19]

We also note that the values of S_F/S_F^0 and $\langle v_F/v_F\rangle$ calculated from (12) and (6) practically agree with those calculated from (7), the difference being only 3%.

D. Measurements over a broad spectral range enabled us to determine the threshold frequency ω_p for interband transitions and the dependence of σ_2 on $\omega - \omega_p$. At helium temperature $\omega_p = 3.7 \times 10^{14}$ sec^{-1} ($\hbar\omega_p = 0.24$ eV); at room temperature $\omega_p = 3.2 \times 10^{14}$ sec^{-1} ($\hbar\omega_p = 0.21$ eV).

Figure 6 shows the dependence of log σ_2 on log $(\omega - \omega_p)$. It is seen that at helium temperature $\sigma_2 \infty (\omega - \omega_p)^{1.0}$ in the large spectral interval $\lambda = 2.4$–5.0μ. At room temperature $\sigma_2 \infty (\omega - \omega_p)^{0.48}$ in the large spectral interval $\lambda = 2.0$–5.8μ. It is

[1)] In the present work we assumed, by analogy with aluminum, that $|V_{111}| < |V_{200}|$. When this inequality is reversed the agreement of the properties becomes even better for the two methods of derivation.

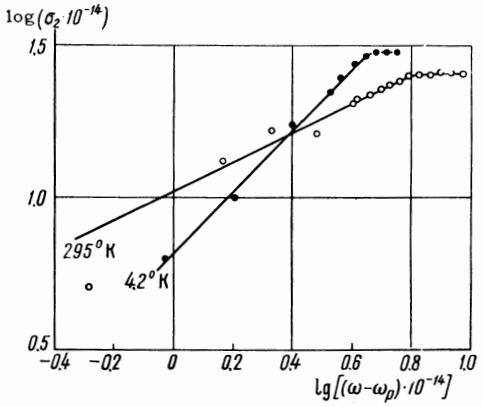

FIG. 6. Dependence of log σ_2 on log $(\omega - \omega_p)$: ●– T = 4.2°K, ○– T = 295°K. The extreme left-hand point, for T = 295°K, was subject to a considerably larger error than the other points and was disregarded when the straight line was fitted.

still not clear to us why the power of the difference term depends on temperature.

6. CONCLUSION

Detailed investigations of the optical properties of indium in the infrared and visible regions, at helium and room temperatures, have been used to determine the properties of conduction electrons and of interband transitions, and to establish a clear relationship between the two sets. The agreement between parameters of the electron structure that were determined by different methods indicates that the established relationship corresponds well to reality.

[1] R. N. Gurzhi and G. P. Motulevich, JETP **51**, 1220 (1966), Soviet Phys. JETP **24**, xxx (1967).

[2] N. W. Ashcroft, Phil. Mag. **8**, 2055 (1963).

[3] J. R. Anderson and A. V. Gold, Phys. Rev. **139**, A1459 (1965).

[4] G. P. Motulevich and A. A. Shubin, Opt. i spektroskopiya **2**, 633 (1957).

[5] A. I. Golovashkin, G. P. Motulevich, and A. A. Shubin, PTÉ No. 5, 74 (1960).

[6] A. I. Golovashkin and G. P. Motulevich, JETP **46**, 460 (1964), Soviet Phys. JETP **19**, 310 (1964).

[7] A. I. Golovashkin and G. P. Motulevich, JETP **47**, 64 (1964), Soviet Phys. JETP **20**, 44 (1965).

[8] C. J. Smithells, Metals Reference Book, 2nd ed., Butterworth's Science Publ., New York and London, 1955.

[9] E. A. Lynton, Superconductivity, Methuen, London and Wiley, New York, 1962.

[10] G. P. Motulevich and A. A. Shubin, JETP **44**, 48 (1963), Soviet Phys. JETP **17**, 33 (1963).

[11] I. N. Shklyarevskiĭ and R. G. Yarovaya, Opt. i spektroskopiya **16**, 85 (1964), Opt. Spectry (USSR) **16**, 45 (1964).

[12] L. Holland, Vacuum Deposition of Thin Films, Chapman and Hall, London, 1956.

[13] G. P. Motulevich, JETP **46**, 287 (1964), Soviet Phys. JETP **19**, 199 (1964).

[14] A. I. Golovashkin and G. P. Motulevich, JETP **44**, 398 (1963), Soviet Phys. JETP **17**, 271 (1963); A. I. Golovashkin, JETP **48**, 825 (1965), Soviet Phys. JETP **21**, 548 (1965).

[15] R. N. Gurzhi, JETP **33**, 451 and 660 (1957), Soviet Phys. JETP 352 and 506 (1958); Dissertation, Physico-tech. Inst., AN, Ukrainian SSR, 1958.

[16] T. Holstein, Phys. Rev. **96**, 535 (1954).

[17] P. J. Lin and J. C. Phillips, Advances in Phys. **14**, 257 (1965).

[18] G. P. Motulevich, JETP **51**, 1918 (1966) issue, p. xxxx.

[19] A. I. Golovashkin, G. P. Motulevich, and A. A. Shubin, JETP **38**, 51 (1960), Soviet Phys. JETP **11**, 38 (1960).

Translated by I. Emin
196